

NANO EXPRESS

Open Access



Silica Cladding of Ag Nanoparticles for High Stability and Surface-Enhanced Raman Spectroscopy Performance

Miaomiao Zhao, Hao Guo, Wenyao Liu, Jun Tang, Lei Wang, Binzhen Zhang, Chenyang Xue, Jun Liu* and Wendong Zhang

Abstract

For high-precision biochemical sensing, surface-enhanced Raman spectroscopy (SERS) has been demonstrated to be a highly sensitive spectroscopic analytical method and Ag is considered to be the best material for SERS performance. Due to the high surface activity of Ag nanoparticles, the high stability of Ag nanostructures, especially in moist environments, is one of the key issues that need to be solved. A method for silica (SiO₂) cladding of Ag nanoparticles (NPs) is demonstrated here for high sensitivity and long-term stability when putted in aqueous solution. The chemically inert, transparent, hydrophilic, and bio-compatible SiO₂ surface acts as the protection layer for the Ag nanoparticles, which can also enhance the Raman intensity to a certain extent. In our study, the Ag@SiO₂ core-shell substrate can detect crystal violet solutions with molar concentrations down to 10⁻¹² M. After 24 h of immersion, the reduction in Raman scattering intensity is about 85 % for sole Ag NP films, compared to 12 % for the Ag coated with a 10-nm SiO₂ layer. This thickness was found to be optimum for Ag@SiO₂ core-shell substrates with long-term stability and high SERS activity.

Keywords: SERS, Ag@SiO₂, Long-term stability, Layer thickness

Background

As a powerful spectroscopic technique, surface-enhanced Raman spectroscopy (SERS) has shown promising applications in surface adsorption, biochemical sensing, and trace-level analysis as a result of its high sensitivity, rapid response, and the advantages of nondestructive detection [1–4]. The mechanism for SERS is mainly attributed to the electromagnetic field enhancement caused by the localized surface plasmon resonance of noble metal nanoparticles (NPs). For isolated metal particles, the electromagnetic enhancement can reach up to 10⁶–10⁷, and when in nanogaps (so-called hotspots), it can reach up to 10¹⁰–10¹¹, because of the electromagnetic coupling between the neighboring metal NPs [5, 6].

Among noble metals, Ag is considered to be one of the most promising candidates for SERS applications due to its low loss in optical frequency and high plasmonic efficiency, as well as its lower cost compared to

other noble metals [7–10]. However, Ag NPs suffer from sulfur contamination, oxidation, and agglomeration in water and the atmosphere, and the biological incompatibility of Ag is obvious, all of which limit their practical application.

Significant efforts have been devoted to improve the chemical stability of Ag NPs, and core-shell nanostructures are one of the most popular methods, which have been reported in literatures [11, 12]. Ag NPs capped with Au [13], graphene [14], and TiO₂ [15] have been reported in recent years. Ma et al. [16] prepared ultrathin (~1.5 nm) Al₂O₃ films by the atomic layer deposition technique on Ag nanorods that can maintain robust morphologies to a temperature of 400 °C. Li et al. [17] reported the use of a single-atom-thick monolayer of graphene for the protection of Ag NPs that can function as a highly stable SERS substrate for nearly 1 month with ambient aerobic exposure.

The capping thickness of the protection layers can be well controlled by the fabrication technology, which has greatly extended the application of Ag-based SERS substrates in different fields. However, a defect of this

* Correspondence: liuj@nuc.edu.cn
Science and Technology on Electronic Test & Measurement Laboratory,
North University of China, Taiyuan, Shanxi 030051, China

coating approach is the tremendous decrease in SERS activity, which is caused by the coating layers that separate the target molecules from the Ag NPs and by the possible morphology changes of the Ag NPs engendered during the coating process. Thus, it is vital to find ways to deposit protective layers which can cap Ag NPs at relatively low temperatures and to precisely control the coating thickness to prohibit the reduction of SERS sensitivity, while still thick enough to be robust towards moist environments.

In this study, Ag NPs were fabricated on 2-in. silicon wafers with a sputtering and vacuum annealing process. We employed inductively coupled plasma-enhanced chemical vapor deposition (ICPECVD) to deposit ultrathin SiO₂ layers that can cap the exposed surface of Ag NPs with a deposition temperature of 60 °C. After deposition of the SiO₂ layer, the SERS performance, as well as the coating influences on the stability of the Ag NPs in a water environment, were investigated. It was found that an ultrathin (10 nm) SiO₂ layer was thick enough to effectively control the distance between the particles to avoid the agglomeration and oxidation even when immersed in water for 15 days. Furthermore, we found that the core-shell structure can improve the SERS performance of Ag substrates when the layer thickness is less than 10 nm.

Methods

Fabrication of Ag NP Films

P-type silicon wafers (2 in. in diameter) were used as the substrate. Ag films were deposited in a high vacuum system equipped with a DC magnetron sputtering source (Qprep500, Mantis, UK). The purity of the Ag target was 99.99 %, and DC magnetron sputtering was performed with a DC power of 46 W, an Ar flow rate of 30 sccm and a chamber pressure of 7.5×10^{-3} Torr. Then, the sample was annealed at 300 °C for 2 h in a high vacuum system of 5×10^{-7} Torr.

Controllable Growth of Silica Layer

The controllable thickness of the SiO₂ coating was realized via the ICPECVD system (SI500D, SENTECH, Germany). For the deposition of the SiO₂ thin films, 130.5 sccm of SiH₄ and mixtures of 13 sccm of oxygen plus 126 sccm of Ar were introduced to the plasma reactor. The final working pressure during deposition conditions was 1.5×10^{-2} Torr, under a deposition temperature of 60 °C. The deposition rate of the SiO₂ thin film was 20 nm/min on average, and the experimental thickness was measured by a stylus profiler (P-7, KLA-Tencor, USA).

Morphology and SERS Characterization

The water contact angle against SiO₂ coating was measured by a contact angle measurement instrument (JGW-360A, Chenghui, China). The morphology of the Ag NPs was characterized by scanning electron microscopy (SUPRA 55

SAPPHIRE, Carl Zeiss AG, Jena, Germany), and the size and density calculations were performed with the assistance of Smile View software.

The stability analysis was conducted by soaking substrates, with and without the cladding layer, into deionized water for 0.5, 1, 5, 10, 24, and 72 h, as well as 15 days. For every period of time, one of the substrates was taken out for testing.

With the distinctive characteristics of Raman peaks, crystal violet (CV) is one of the most commonly used probe molecules in surface-enhanced Raman scattering. In addition, CV is listed as a banned drug of aquaculture by many countries for its high toxicity, high persistence, and cancer-causing peculiarities; thus, it is a good choice for the trace detection experiments [18, 19]. We describe it by the formula of C₂₅H₃₀ClN₃, and the relative molecular mass is 407.99. By diluting different masses of solid CV with deionized water, different molar concentrations of CV solution were prepared. All the experiments were performed in a thousand level clean room with a temperature of 20 °C and a relative humidity of 60 %.

SERS characterization was performed after immersion of the samples in CV solutions. The samples were excited using a 514.5-nm laser line from the Raman microscope system (Invia, Renishaw, UK) with an excitation power beam of 5 mW.

Results and Discussion

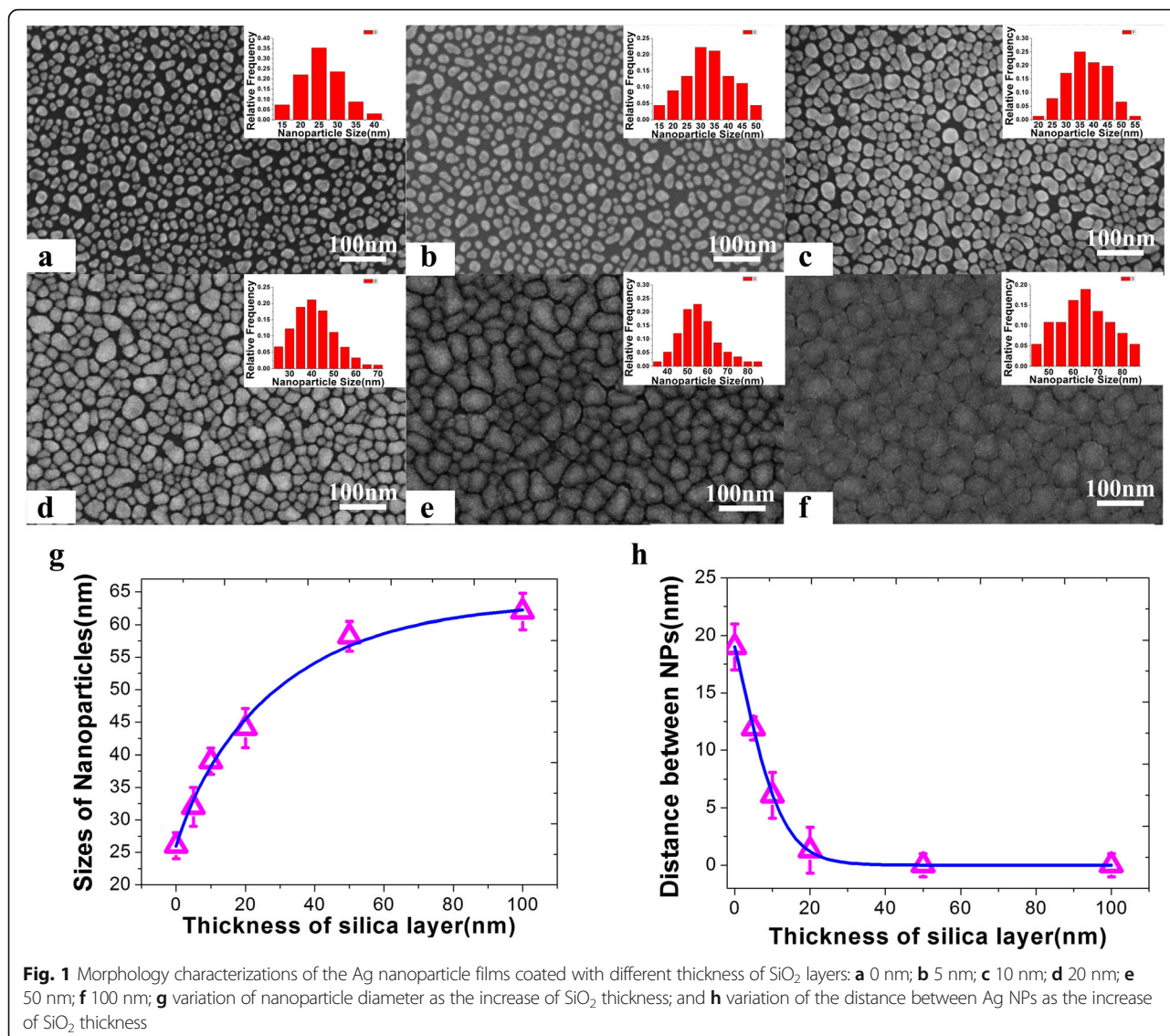
Morphology Characterization of Ag@SiO₂ Nanostructure

Different film thickness of the SiO₂ layers can be achieved by controlling the SiO₂ deposition time, and the morphology of the Ag@SiO₂ nanostructure was characterized by scanning electron microscopy (SEM), as shown in Fig. 1 and Additional file 1: Figure S1. The corresponding energy spectrum shows the coincident results (Additional file 1: Figure S2). From the characterization results, as shown in Fig. 1g, h, the mean diameters of Ag@SiO₂ nanostructures were 26 ± 2.3 , 32 ± 3.6 , 39 ± 2 , 44.1 ± 3.3 , 58.2 ± 2.5 , and 62.2 ± 3.2 nm, calculated with the assistance of Smile View software, and the interparticle distance decreased from 19 to 0 nm.

SERS Characterization of Ag@SiO₂ Core-Shell Nanostructure and Research on the Enhancement Mechanism

The samples were immersed into 10^{-6} M CV solution, which acted as the probe molecule for 30 min, and then dried in air. The SERS activity of the substrates was tested with the Raman microscope system, and the results are shown in Fig. 2.

There exist various bands for CV at around 913 cm⁻¹, attributed to radial aromatic ring skeleton vibrating. The band at 1174 cm⁻¹ is related to the C–H bending vibration, while the band at 1620 cm⁻¹ is related to the C=C stretching vibration. As shown in Fig. 2a, the thickness



of 10 nm acts as the turning point for Raman intensity, and the calculated results reveal that Ag NPs coated with the appropriate shell thickness can improve the sensitivity of SERS active substrates. The highest enhancement in Raman scattering is threefold for the 10-nm shell compared to the uncoated Ag NPs. Besides, the reproducibility of the Ag@SiO₂ core-shell structure is good by comparing the SERS performance of 12 different 10-nm SiO₂-coated substrates (Additional file 1: Figure S3).

To further characterize the SERS sensitivity of Ag@SiO₂ with the SiO₂ shell of 10 nm, we immersed the substrates in different concentrations of CV solution. As shown in Fig. 2c, we can find that quite high sensitivity was achieved with the Ag@SiO₂ structure, which can detect CV concentrations down to 10⁻¹² M with the signal-to-noise ratio of 6.3 dB. Finally, the enhancement factor (EF) was used to characterize the

SERS enhancement of Ag@SiO₂ nanostructures. It was calculated according to the equation as Leem [20] described:

$$EF = \frac{I_{sers}/C_{sers}}{I_{sol}/C_{sol}} \tag{1}$$

where I_{sers} and I_{sol} are the normalized Raman peak intensities of the CV molecules absorbed on the SERS substrate and the reference solution of the selected Raman peak at 1620 cm⁻¹, respectively. C_{sers} is the molar concentration of the CV on SERS substrates, and C_{sol} is the molar concentration of the reference CV solution. According to the results of our experiment, the I_{sers} and I_{sol} are equal to 90,000 and 136, respectively, and the C_{sers} and C_{sol} are equal to 10⁻⁶ and 10⁻² M, respectively. Therefore, the EF of our Ag@SiO₂ substrate is 6.6 × 10⁶.

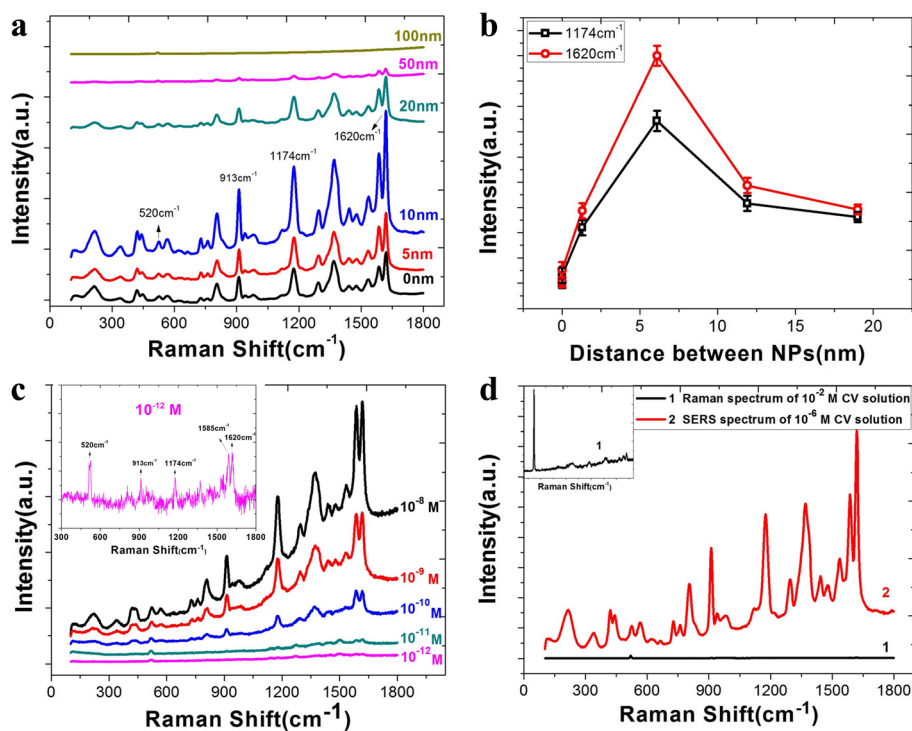


Fig. 2 SERS characterizations of Ag@SiO₂ substrates. **a** SERS spectra of CV on Ag@SiO₂ substrates with the thickness of SiO₂ layers vary from 0 to 100 nm. **b** Spectrum intensity calculations of CV at 1174 and 1620 cm⁻¹ based on the interparticle distance. **c** SERS spectra of CV absorbed on Ag@SiO₂ substrate after immersed in different concentrations of CV solution. **d** Normal Raman spectrum of 10⁻² M CV solution on silicon wafer (1) and SERS spectrum of 10⁻⁶ M CV solution on Ag@SiO₂ substrate (2)

We believe there were three reasons that a SiO₂ layer contributes to a higher SERS activity. Firstly, the high refractive index of SiO₂ layer can confine the light, just like the optical fiber used in the optical communication. Secondly, the multiscattering processes of the light that scattered back and forth at the two curved surfaces of SiO₂ layers will contribute to a larger enhancement factor in the cavity. Thirdly, the interference of the scattered light from the inner and outer interfaces can diminish the optical field inside the layer, and due to the energy conservation, a relatively larger enhanced field is focused at the outer surface of SiO₂ layer [21, 22]. Thus, a huge SERS enhancement especially in the cavity between coated Ag NPs can be obtained, which also have been proved by the finite-difference time-domain (FDTD) simulations, as shown in Fig. 3.

In addition, we believe that the high hydrophilic SiO₂ coating can aggrandize the adsorption quantity of CV molecules on the surface of substrates, which will have an effect on the SERS enhancement to a certain extent [23]. We herein assessed the hydrophilic character with water contact angles. As substantiated by the shift in dynamic contact angle (Additional file 1: Figure S4), a significant increase in surface hydrophilicity of the

Ag@SiO₂ substrates was found. To quantitatively express the impact of the mesoporous structure and hydrophilicity of SiO₂ layer on the SERS enhancement, we contrasted the Raman intensity of bare Si substrates and Si@SiO₂ substrate. The enhancement factor here can be calculated according to the Eq. (1) too, and the result is 6.65.

Meanwhile, as a surface-sensitive technique, SERS performance decays exponentially according to the distance between target molecules and SERS substrates. Thus, the increase in SiO₂ layers separates the probing molecules from Ag NPs, resulting in a sharp reduction in Raman intensity [24].

Stability Analysis of Ag@SiO₂ Core-Shell Substrates

To characterize the long-term stability of Ag@SiO₂ core-shell nanostructures in aqueous solution sensing applications, we put the Ag NP films coated with 0, 10, and 20 nm SiO₂ layers into deionized water for comparison experiments. At the soaking times of 0.5, 1, 5, 10, 24, and 72 h and 15 days, one of the substrates was taken out and then immersed in a 10⁻⁶ M CV solution for 10 min. The morphology of the NPs on three kinds of substrates after the immersion process were characterized by SEM. The SEM images (Additional file 1: Figure S5) showed that Ag

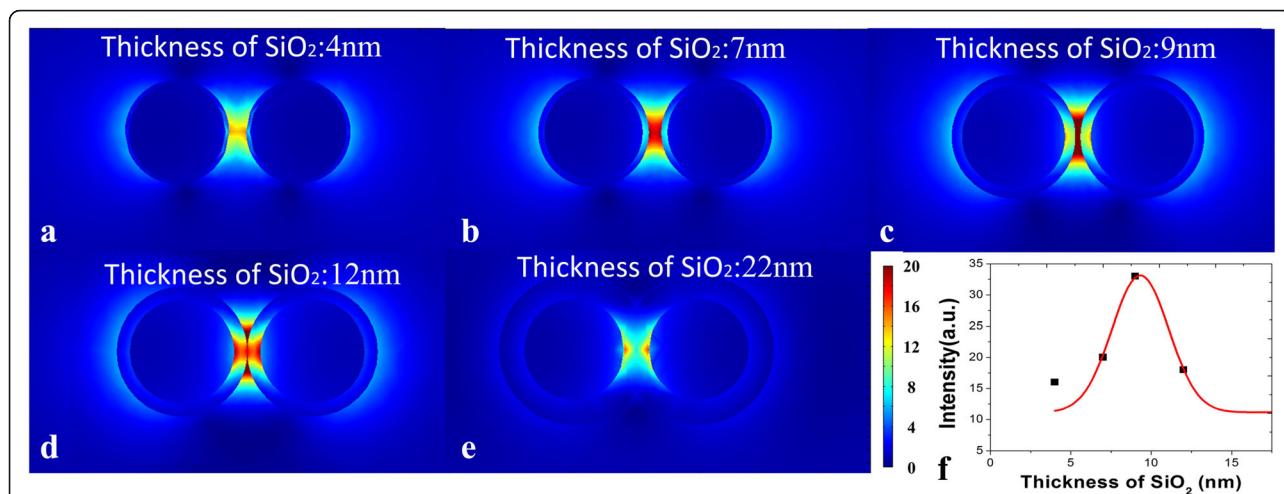


Fig. 3 FDTD simulation results for the intensity trend along with the change of spacing. **a** Ag nanoparticles coated with 5 nm SiO₂, the distance between Ag@SiO₂ nanostructures is 14 nm. **b** Distance between Ag@SiO₂ nanostructures is 10 nm. **c** Distance between Ag@SiO₂ nanostructures is 4 nm. **d** Distance between Ag@SiO₂ nanostructures is 0 nm. **e** Ag nanoparticles coated with 20 nm SiO₂; here, we denoted the distance between Ag@SiO₂ nanostructures as -16 nm. **f** Variation of the SERS intensity along with the spacing between nanoparticles

NP films can be greatly destroyed when exposed to an aqueous solution. After soaking for 0.5 h, agglomeration appeared and almost one third of the NPs were removed, and after 10 h, only a few residues of the Ag NPs can be found which were also strongly agglomerated. Apparently, the stability of Ag NP films is very poor when soaking in the aqueous solution, which can greatly restrict the performance of the SERS activity. Inversely, Ag NPs coated with a 10 nm, as well as a 20-nm SiO₂ layer, can still remain the morphology even after 24 h of immersion, and the agglomeration of NPs was not discovered after soaking for 15 days. It is obvious that the SiO₂ layer can protect Ag NPs with a thickness of 10 nm (Fig. 4).

The effect on the SERS activity of substrates during the immersion process was also characterized by Raman microscope system, and the result is shown in Fig. 5. From the figures, we can find that, with the increased

soaking time, the Raman intensity of CV absorbed on Ag@SiO₂ substrates is stable, while for bare Ag NP films, the intensity decreasing sharply. After 24 h of immersion, the decrease in Raman spectrum intensity is about 85 % for bare Ag NP films, compared to 12 % for the Ag NP films with a 10-nm SiO₂ layer, and 15 % for Ag NP films with a 20-nm SiO₂ layer (Fig. 5d).

From the results, it can be concluded that SiO₂-coated metallic NP films can greatly increase the long-term stability compared to bare Ag NP films, especially when the structures are exposed to aqueous solution.

Applications of Ag@SiO₂ Core-Shell Substrates

For the aqueous solution sensing applications, Ag@SiO₂ substrates are further developed with better sensitivity and selectivity through chemical functionalization. We

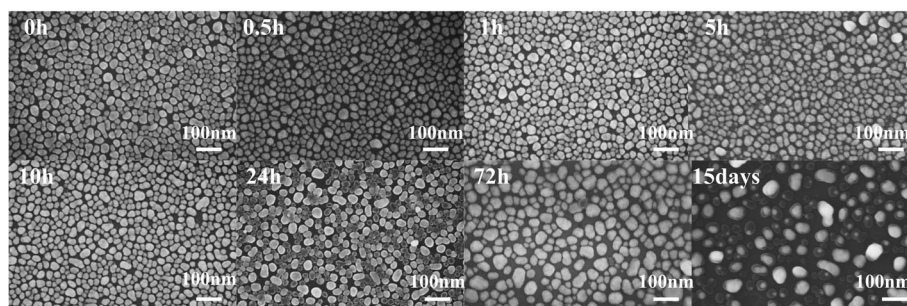


Fig. 4 Morphology characterizations of the Ag@SiO₂ nanostructures after immersing in deionized water for 0, 0.5, 1, 5, 10, 24, and 72 h and 15 days with the thickness of SiO₂ is 10 nm

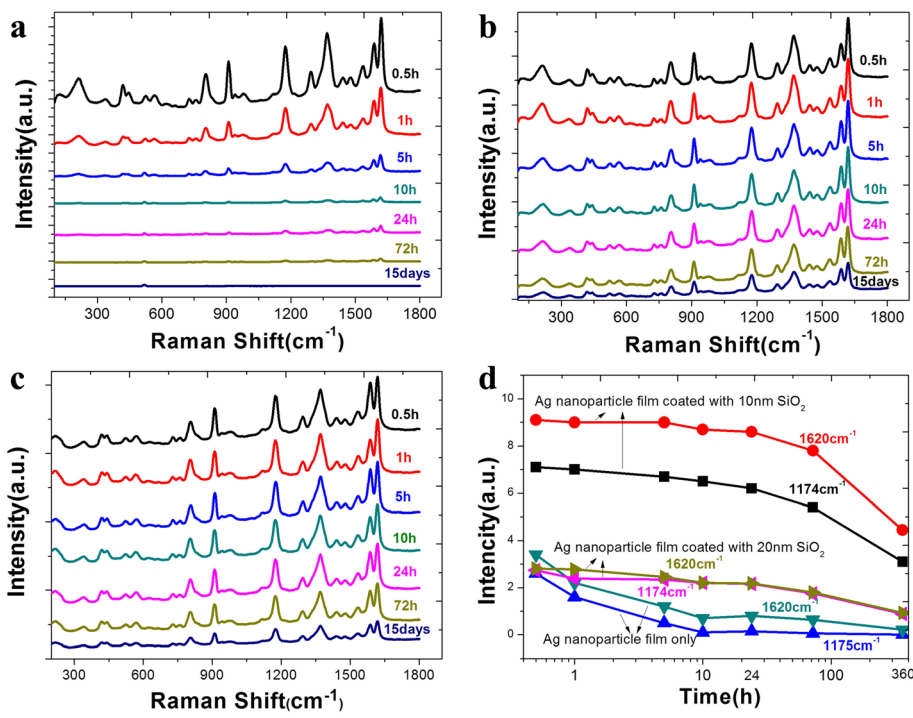


Fig. 5 Characterization of SERS-activity, Raman spectra of CV on **a** bare Ag NP films; **b** Ag NP films coated with 10-nm SiO₂ layer; **c** Ag NP films coated with 20-nm SiO₂ layer after soaking for different time; and **d** the intensity curves of CV at 1174 and 1620 cm⁻¹ absorbed on the substrates with and without SiO₂

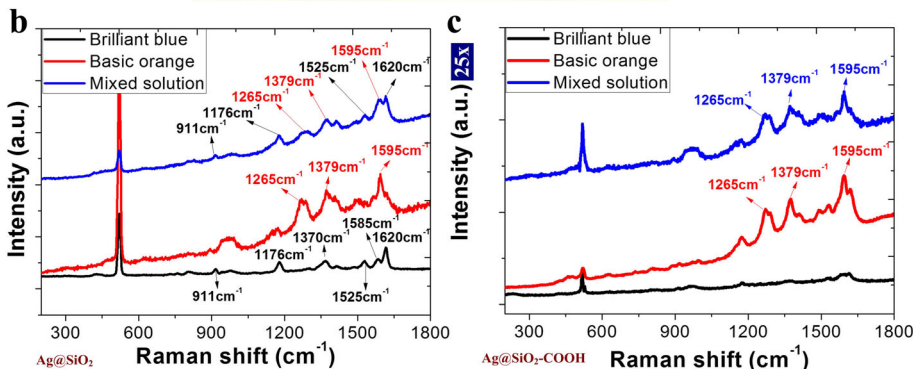
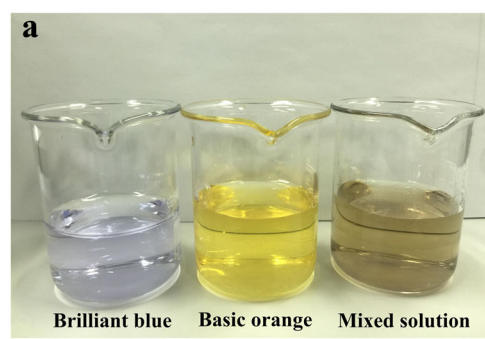


Fig. 6 a The dilute solutions of brilliant blue (BB), basic orange (BO), and the mixed solution of BB and BO, respectively. **b** The Raman spectra of Ag@SiO₂ substrate after immersing in the three kinds of solutions. **c** The Raman spectra of Ag@SiO₂-COOH substrate after immersing in the three kinds of solutions

found that a negatively charged surface could be achieved by $-COOH$ functionalization.

Solutions of the food additives brilliant blue (BB) and basic orange (BO) were used. BB molecules in the solution are negatively charged, and BO molecules carry two amino groups. The molarity of BB and BO solutions are 10^{-6} M.

We immersed the $Ag@SiO_2$ as well as the $Ag@SiO_2-COOH$ substrates in the dilute solutions of BB, BO, and the mixed solution of BB and BO, respectively. The Raman spectra of the three samples are shown in Fig. 6. From Fig. 6b, we can find that both molecules on the nonfunctionalized substrate were detected. Different phenomena were observed with the negatively charged, functionalized substrate (Fig. 6c). In the solutions of BB and the mixed solution of BB and BO, the Raman band due to BB nearly disappeared. This result indicates that the sensitivity to positively charged molecules is improved with the negatively charged SiO_2 surface and decreased to negatively charged molecules.

The high sensitivity to the specific molecule gives the potential applications of $Ag@SiO_2$ in accurate biochemical sensing.

Conclusions

In this study, a method for SiO_2 cladding of Ag NPs with long-term stability in aqueous solution was presented and demonstrated. The ICPECVD-grown SiO_2 layer can suppress the oxidation of Ag NPs effectively and prevent the aggregation and deformation of the particles from occurring. Furthermore, the SERS activity of Ag NP films can be increased by optimizing the thickness of the SiO_2 dielectric layer that can detect CV concentrations down to 10^{-12} M, and the EF of $Ag@SiO_2$ substrates in our experiment can reach up to 6.6×10^6 . This work thus provides a straightforward and cost-effective approach to fabricating Ag-based SERS substrates with unprecedented stability and gives us a reliable way to apply Ag nanostructures in the field of solution composition detection. Also, as a bio-compatible material, a SiO_2 coating of the nanostructure for highly sensitive biochemical sensing can be further applied for various biosensor applications.

Additional file

Additional file 1: Figure S1. The cross-sectional views of $Ag@SiO_2$ nanostructures with the thickness of SiO_2 layers vary from 0 to 50 nm. **Figure S2.** The corresponding energy spectrum of $Ag@SiO_2$ nanostructures with the thickness of SiO_2 layers vary from 0 to 50 nm. **Figure S3.** Characterization of the reproducibility of $Ag@SiO_2$ nanostructure (a) Raman spectra of CV on different $Ag@SiO_2$ substrates (b). The intensity curves of CV at 1174 and 1620 cm^{-1} absorbed on the substrates. **Figure S4.** A water droplet falling on (a) the Ag film; (b) the $Ag@SiO_2$ film; (c) Raman spectra of CV molecules on Si (1)/Si coated with 10-nm SiO_2 wafer (2). **Figure**

S5. Morphology characterizations of the $Ag@SiO_2$ nanostructures after immersing in deionized water for 0, 0.5, 1, 5, 10, 24, and 72 h and 15 days with the thicknesses of SiO_2 are (a) 0 nm (b) 10 nm, and (c) 20 nm. (DOC 19191 kb)

Acknowledgements

We acknowledge the financial support from the Natural Science Foundation of China (51225504, 61127008, 61571405, and 110248-28140) and the program for the top young academic leaders of higher learning Institutions of Shanxi.

Authors' Contributions

MZ and HG contributed equally to this work, performed the most measurements, analyzed the data, and wrote the main manuscript text. JL and LW prepared the samples and performed the SEM and EDS measurements. JT and WL designed the experiment and contributed to the manuscript writing. BZ modified the manuscript. CX and WZ offered helpful suggestions in the study. All authors read and approved the final manuscript.

Competing Interests

The authors declare that they have no competing interests.

Received: 10 May 2016 Accepted: 31 August 2016

Published online: 15 September 2016

References

- Liu J, Meng GW, Li ZB, Huang ZL, Li XD (2015) Ag-NP@Ge-nanotaper/Si-micropillar ordered arrays as ultrasensitive and uniform surface-enhanced Raman scattering substrates. *Nanoscale* 7:18218–18224
- Gai SL, Yang PP, Li CX, Wang WX, Dai YL, Niu N et al (2010) Synthesis of magnetic, up-conversion luminescent, and mesoporous core-shell-structured nanocomposites as drug carriers. *Adv Funct Mater* 20:1166–1172
- Preciado FS, Wheeler DA, Tran TM, Tanaka Z, Jiang CY, Barboza FM et al (2011) SERS spectroscopy and SERS imaging of *Shewanella oneidensis* using silver nanoparticles and nanowires. *Chem Comm* 47:4129–4131
- Shafer P, Karen E, Haynes CL, Glucksberg MR et al (2003) Toward a glucose biosensor based on surface-enhanced Raman scattering. *J Am Chem Soc* 125:588–593
- Zeman EJ, Schatz GC (1987) An accurate electromagnetic theory study of surface enhancement factors for silver, gold, copper, lithium, sodium, aluminum, gallium, indium, zinc, and cadmium. *J Phys Chem* 91:634–643
- Le Ru EC, Blackie E, Meyer M, Etchegoin PG (2007) Surface enhanced Raman scattering enhancement factors: a comprehensive study. *J Phys Chem C* 111:13794–13803
- Rycenga M, Cobley CM, Zeng J, Li WY, Moran CH, Zhang Q (2011) Controlling the synthesis and assembly of silver nanostructure for plasmonic application. *Chem Rev* 111:669–712
- Xia XH, Zeng J, Zhang Q, Moran CH, Xia YN (2012) Recent developments in shape-controlled synthesis of silver nanocrystals. *J Phys Chem C* 116:47–56
- Hou H, Wang P, Zhang J, Li CP, Jin YD (2015) Graphene oxide-supported Ag nanoplates as LSPR tunable and reproducible substrates for SERS applications with optimized sensitivity. *ACS Appl Mater Interfaces* 7:18038–18045
- Ma Y, Qu Y (2012) A simple approach towards uniform spherical Ag-like nanoparticles. *Nanoscale* 4:6–9
- Liu K, Bai YC, Zhang L, Yang ZB, Fan QK, Zheng HQ (2016) Porous Au-Ag nanospheres with high-density and highly accessible hotspots for SERS analysis. *Nano Lett* 16:3675–3681
- Liu YT, Zhou J, Wang BB, Jiang T, Ho H, Petti L et al (2015) Au@Ag core-shell nanocubes: epitaxial growth synthesis and surface-enhanced Raman scattering performance. *Phys Chem Chem Phys* 17:6819–6826
- Gao CB, Lu ZD, Liu Y, Zhang Q, Chi MF, Cheng Q et al (2012) Highly stable silver nanoplates for surface plasmon resonance biosensing. *Angew Chem Int Ed* 51:29–33
- Gao N, Yang T, Liu T, Zou Y, Jiang J (2015) Graphene oxide wrapped individual silver nanocomposites with improved stability for surface-enhanced Raman scattering. *RSC Adv* 5:55801–55807
- Hirakawa T, Kamat PV (2005) Charge separation and catalytic activity of $Ag@TiO_2$ core-shell composite clusters under UV-irradiation. *J Am Chem Soc* 127:28–34

16. Ma LW, Huang Y, Hou MJ, Xie Z, Zhang ZJ (2015) Silver nanorods wrapped with ultrathin Al_2O_3 layers exhibiting excellent SERS sensitivity and outstanding SERS stability. *Sci Rep* 5:12890
17. Li XY, Li J, Zhou XM, Ma YY, Zheng ZP, Duan XF et al (2014) Silver nanoparticles protected by monolayer graphene as a stabilized substrate for surface enhanced Raman spectroscopy. *Carbon* 66:713–719
18. Senapati S, Srivastava SK, Singh SB, Kulkarni AR (2014) SERS active Ag encapsulated Fe@SiO_2 nanorods in electromagnetic wave absorption and crystal violet detection. *Environ Res* 135:95–104
19. Zhang KB, Zeng TX, Tan XL, Wu WD, Tang YJ, Zhang HB (2015) A facile surface-enhanced Raman scattering (SERS) detection of rhodamine 6G and crystal violet using Au nanoparticle substrates. *Appl Surf Sci* 347:569–573
20. Leem J, Kang HW, Ko SH, Sung HJ (2014) Controllable Ag nanostructure patterning in a microfluidic channel for real-time SERS systems. *Nanoscale* 6:2895–2901
21. Liu FX, Tang CJ, Zhan P, Chen Z, Ma HT, Wang ZL (2014) Released plasmonic electric field of ultrathin tetrahedral-amorphous-carbon films coated Ag nanoparticles for SERS. *Sci Rep* 4:4494
22. Xu HX (2004) Theoretical study of coated spherical metallic nanoparticles for single-molecule surface-enhanced spectroscopy. *Appl Phys Lett* 85:5980–5982
23. Kotte L, Althues H, Mader G, Roch J, Kaskel S, Dani I et al (2013) Atmospheric pressure PECVD based on a linearly extended DC arc for adhesion promotion applications. *Surf Coat Technol* 234:8–13
24. Gong JX, Li GD, Tang ZY (2012) Self-assembly of noble metal nanocrystals: fabrication, optical property, and application. *Nano Today* 7:564–585

Submit your manuscript to a SpringerOpen® journal and benefit from:

- Convenient online submission
- Rigorous peer review
- Immediate publication on acceptance
- Open access: articles freely available online
- High visibility within the field
- Retaining the copyright to your article

Submit your next manuscript at ► springeropen.com
